ALIEN EARTHS

Which Nearby Planetary Systems Are Likely to Host Habitable Planets and Life?

MONTHLY NEWSLETTER

July 2026

Alien Earths is part of NASA's Nexus for Exoplanetary System Science program, which carries out coordinated research toward the goal of searching for and determining the frequency of habitable extrasolar planets with atmospheric biosignatures in the Solar neighborhood.

Our interdisciplinary teams include astrophysicists, planetary scientists, cosmo chemists, material scientists, chemists, biologists, and physicists.

The Principal Investigator of Alien Earths is Daniel Apai (University of Arizona). The projects' lead institutions are The University of Arizona's Steward Observatory and Lunar and Planetary Laboratory.

For a complete list of publications, please visit the **AE Library** on the SAO/NASA Astrophysics Data System.

Recent Publications

The Effect of External Photoevaporation on the Disk Fraction in M17

Most Rocky Sub-Neptunes are Molten: Mapping the Solidification Shoreline for Gas Dwarf Exoplanets

The K-dwarfs Survey — I. Four Validated Planets from the Radius Valley to the Neptune Desert

Molecular Similarity and Water Diversity in Coeval Binary Disks: JWST/MIRI Observations of Sz 65 and Sz 66

Volatile-rich Evolution of Molten Super-Earth L98-59 d

Hidden Gems in TESS: SHERLOCK Finds Two New Rocky Planets Around Nearby M Dwarfs

Evidence for Systematically Larger Dust Grains in Upper Scorpius Relative to Taurus Disks

A Panchromatic JWST Spectrum of a Giant Starspot on the Fully Convective M Dwarf TOI-3884

From Young to Older Disks: JWST/MIRI Evidence for Fading Molecular Emission and Hints for Elevated C/O in Upper Scorpius

Probabilistic Spectral Reconstruction of Trans-Neptunian Objects from Sparse Photometry: A Framework for Taxonomy, Survey Optimization, and Outlier Detection

Coupled atmosphere Interior model Intercomparison (CHILI) – Protocol Version 1.0: A CUISINES Intercomparison Project of Magma Ocean Models

A Gem System with a Lava World and a Habitable Zone Sub-Neptune Orbiting TOI-1752

The Goldilocks Problem for Detecting Water in Terrestrial Planets: Constraining Water Abundances in the Mid-infrared with LIFE

NSF-DOE Vera C. Rubin Observatory Observations of Interstellar Comet 3I/ATLAS (C/2025 N1)

The Effect of External Photoevaporation on the Disk Fraction in M17

Samuel Millstone, Megan Reiter, Morten Andersen, Thomas J. Haworth, Dominika Itrich, Anna McLeod, Richard J. Parker, Andrew Winter, and Peter Zeidler

Astrophysical Journal, Volume 1005, Number 1

A major obstacle to improving models of planet formation is understanding how the local environment influences the lifetimes of the disks in which planets form. The spread in observed disk lifetimes is caused by effects both observational (e.g., target selection, survey sensitivity) and physical (e.g., disk destruction by internal and external photoevaporation); however, the degree to which each plays a role remains poorly constrained. Isolating the impact of external photoevaporation on disk lifetimes benefits from the inclusion of low-mass ($\lesssim 0.5\ M_{\odot}$) young stellar objects (YSOs), for which this effect is expected to be most significant. In this work, we measure the inner disk fraction from *JHK* excess in the ∼6000 $M_{\odot}$, ∼1 Myr-old star-forming region (SFR) M17. Using the High Acuity Wide-field *K*-Band Imager (or HAWK-I) on the Very Large Telescope, we perform a deep photometric survey of an ∼8’ x 8’ field toward the region. The ∼4 times greater sensitivity and ∼2−3 times higher resolution compared to previous surveys of M17 reveal 10,339 sources. We select cluster members using the Massive Young Star-Forming Complex Study in Infrared and X-ray (or MYStIX) catalog and find a disk fraction of 28% ± 2%—the first X-ray-selected disk fraction measurement in M17 to include low-mass YSOs, and only the second such measurement in any high-mass SFR. After correcting for observational biases, we find no correlation between disk fraction and incident UV flux within M17, likely due to dynamical mixing within the region. However, when compared with other regions of similar age, we find lower disk fractions in regions with stronger UV fields, suggesting that external photoevaporation decreases the average disk lifetime.

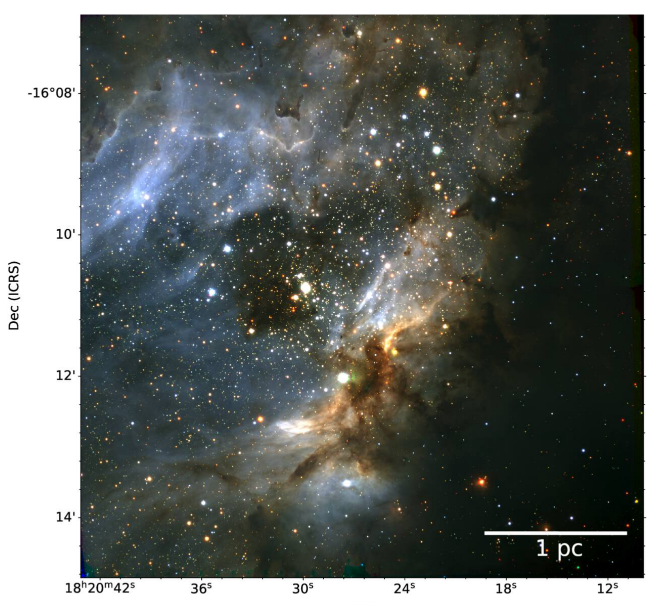

Figure 1. Near-IR JHKs image of M17 from VLT/HAWK-I. More than 10,000 sources are detected down to J-band magnitude of ∼19.5−21 with an angular resolution of ∼0.3”−0.5 “(see Table 1). The O4–O4 double binary CEN 1, located at $18^h20^m29^s.8$, -16°10′45", marks the center of the region, and note the IR-dark cloud directly to the east/southeast. Red: 2.15 μm; green: 1.62 μm; blue: 1.26 μm.

Most Rocky sub-Neptunes are Molten: Mapping the Solidification Shoreline for Gas Dwarf Exoplanets

Robb Calder, Oliver Shorttle, Harrison Nicholls, Tim Lichtenberg, Claire Marie Guimond

Monthly Notices of the Royal Astronomical Society, Volume 549, Issue 3, July 2026, stag1007

Sub-Neptunes are the most common type of detected exoplanet, yet their observed masses and radii are degenerate with several interior structures. One possibility is that sub-Neptunes have silicate/iron interiors and H_2 – dominated atmospheres (μ < 3.8 g mol^{-1}), i.e. they are 'gas dwarfs.' If gas dwarfs have molten interiors, interactions between their magma oceans and atmospheres will produce distant observational signatures. These signatures may break the degeneracy in interior structure, while providing insight into their interior processes, history, and population trends. We expect all such planets are born molten, but under what conditions to they remain molten today? We use the coupled interior-climate evolution model, PROTEUS, to estimate the 'solidification shoreline': the instellation flux boundary (as function of stellar $T_{\rm eff}$) that separates molten gas dwarfs from solidified ones. Our results show that 98 percent of detected sub-Neptunes occupy a region of parameter space consistent with their having permanent magma oceans, if they are gas dwarfs. While mantle fO_2 and bulk volatile C/H ratio both influence magma ocean cooling, planets with oxidizing mantles and carbon-rich atmospheres are likely to have high mean-molecular weight atmospheres (μ > 3.8 g mol^{-1}) and are thus outside the scope of this study. Therefore, most detected sub-Neptunes, if they are gas dwarfs, have permanent magma oceans. This result motivates further research into the interactions between molten interiors and overlying atmospheres, and campaigns to identify unambiguous signatures of these interactions.

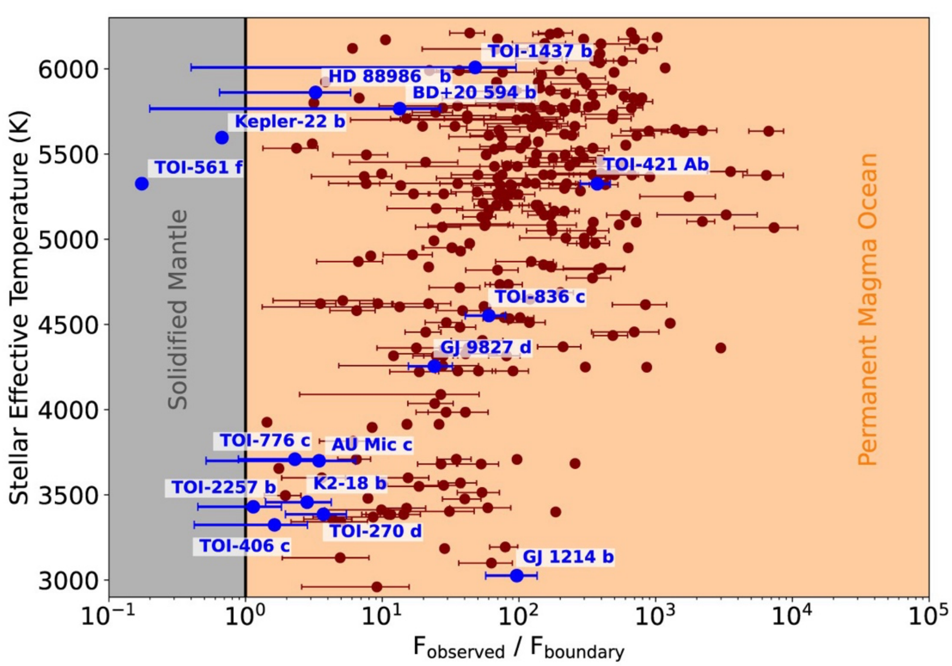

Figure 1 – Right: *Ratio of the observed installation flux of detected sub-Neptunes ($F_{observed}$) to the instellation flux required for them to be on their appropriate solidification shoreline ($F_{boundary}$) as a function of host star effective temperature. Errors in $F_{observed}/F_{boundary}$ =1, corresponding to a planet located on the solidification shoreline, is shown. Sub-Neptunes for which there exist published JWST transmission spectra as well as those in the solidified mantle region are shown in blue, and those without JWST transmission spectra are shown in maroon.*

The K-dwarfs Survey — I. Four Validated Planets from the Radius Valley to the Neptune Desert

G. Morello, A. Peláez-Torres, F. J. Pozuelos, M. Dévora-Pajares, F. Murgas, J.P. de Leon, B. Rojas-Ayala, Bieryla, A. K. Barkaoui, S. Yalçinkaya, Ö. Baştürk, B.V. Rackham, A. Burgasser, E. Pallé, N. Narita, R. Varas, P.J. Amado, N. Abreu García, I. Bonilla-Mariana, Y. Calatayud-Borras, E. Esparza-Brges, G. Fernández-Rodríguez, I. Fukuda, A. Fukui, A. García-Serra, S. Geraldía-González, J. González-Rodríguez, Y. Hayashi, K. Ikuta, K. Isogai, Y. Kawai, K Kawauchi, P. Klagyivik, J. Korth, G. Lacedelli, F. Libotte, J.H. Livingston, P. Montañés-Rodríguez, M. Mori, J. Orell-Miquel, H. Parviainen, M. Sánchez-Benavente, N. Watanave, K.A. Collins, R.P. Schwarz, C. Stockdale, F.P. Wilkin, R. Zambelli, M.E. Everett, D.R. Ciardi, C.A. Clark, M.B. Lund, M. Timmermans, E. Ducrot, M.J. Hooton, P.P. Pedersen, A. Burdanov, A. H. M. J Triaud, J. de Wit, F. Grau Horta, G. Domènech-Rams, E. Herrero, J. Lopesino, B.O. Demory, M. Gillon, Y. Gómez Maqueo Chew, Al Khandelwal, M. Lendl, M. Pichardo Marcano, I. Plauchu-Frayn, D. Queloz, U. Schroffenegger, F. Zong Lang, J.F. Kielkopf, H.P. Osborn, A. Krenn, Y. Alibert, T. Wilson, A. Deline, A. Fortier, P.F.L. Maxted, M.N. Günther

Monthly Notices of the Royal Astronomical Society, Volume 549, Issue 3, July 2026, stag183

Sub-Neptune-sized exoplanets are the most common class discovered by transit surveys, yet their detailed exploration has just begun. Their demographics have inspired models of planetary formation and evolution, though the sample is naturally biased toward the predominance of M-dwarf systems, which provide more favourable observing conditions. We aim to validate the planetary nature of four candidates identified by the Transiting Exoplanet Survey Satellite (TESS) orbiting K-dwarf stars: TOI-2133.01, TOI-5734.01, TOI-5938.01, and TOI-7009.01. We used photometric, spectroscopic, and high-resolution imaging data from the TESS Follow-up Observing Programme with well-established and cutting-edge tools for validating the planetary nature of the candidates. We validate all four candidates and determine their system parameters. TOI-2133 b and TOI-5734 b lie near the upper edge of the radius valley, while TOI-5938 b and TOI-7009 b are at the boundary of the Neptune desert, making them rare additions to the known sub-Neptune population. The planets are suitable for precise mass measurements and atmospheric characterization with current facilities, making them benchmark targets for testing formation and evolution models around K-dwarf hosts, a population less accessible than the typical M-dwarf systems.

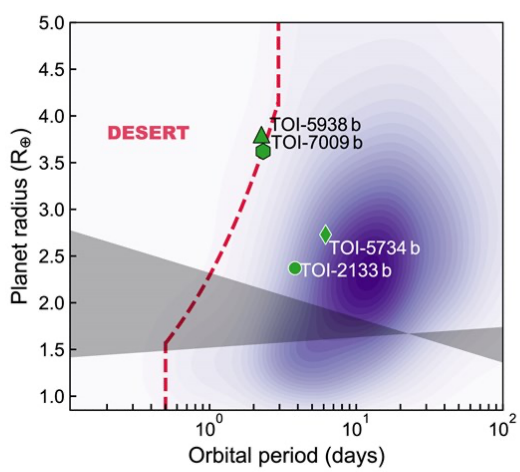

Figure 4.
Location of the validated new planets TOI-2133 b (circle), TOI-5734 b (diamond), TOI-5938 b (triangle), and TOI-7009 b (hexagon). The different density levels and the corresponding colourmap indicate planet occurrence, with purpler regions being more populated and whiter regions less populated. The red dashed line marks the boundary of the Neptune desert, as defined by A. Castro-González et al. (2024). The black-shaded region shows the radius valley of sub-Neptune exoplanets around low mass stars measured by R. Cloutier & K. Menou (2020) and the radius valley for exoplanets around Sun-like stars measured by C. F. Martinez et al. (2019), scaled to low mass stars by R. Cloutier & K. Menou (2020).

Molecular Similarity and Water Diversity in Coeval Binary Disks: JWST/MIRI Observations of Sz 65 and Sz 66

Jinghuai Yao, Ke Zhang, Andrea Banzatti, Naman S. Bajaj, Ilaria Pascucci, James Miley, Geoffrey A. Blake, Colette Salyk, John M. Carpenter, Paola Pinilla, Lucas A. Cieza, Miguel Vioque, and Benoît Tabone

The Astrophysical Journal, Volume 1005, Number 1

We present JWST/MIRI Medium Resolution Spectrometer spectra of the wide-separation (projected separation = 980 au) binary protoplanetary disks Sz 65 (K7; 0.68 $M_\odot$) and Sz 66 (M3; 0.30 $M_\odot$), reduced using the uniform pipeline of the JWST Disk Infrared Spectral Chemistry Survey. Both disks show rich molecular emission, including H_2O, CO_2, HCN, C_2H_2, and OH. The scaled spectra of the two disks exhibit remarkably similar H_2O, CO_2, and HCN line emission in the 13–18 μm region, with the only notable difference being stronger C_2H_2 emission in the primary (Sz 65). Beyond 18 μm, the difference in H_2O line emission between the two disks increases. Both the flux ratios and the slab-model-derived mass ratios of cold to hot H_2O (~200 to ~750 K) and warm to hot H_2O (~450 to ~750 K) are significantly higher in the secondary (Sz 66). Because binary stars share nearly the same age and metallicity, and as both disks appear compact in millimeter emission (<30 au), we suggest that the excess cold H_2O in the secondary is best explained by its unstructured dust disk, in contrast to the primary, which shows gaps at 6 and 20 au. The enhanced cold water in the secondary is consistent with efficient pebble drift across the water snow line and increased H_2O vapor from the sublimation of icy mantles. Our results demonstrate that wide-separation binaries can serve as powerful control samples for isolating the impact of individual disk properties on inner-disk chemistry and evolution.

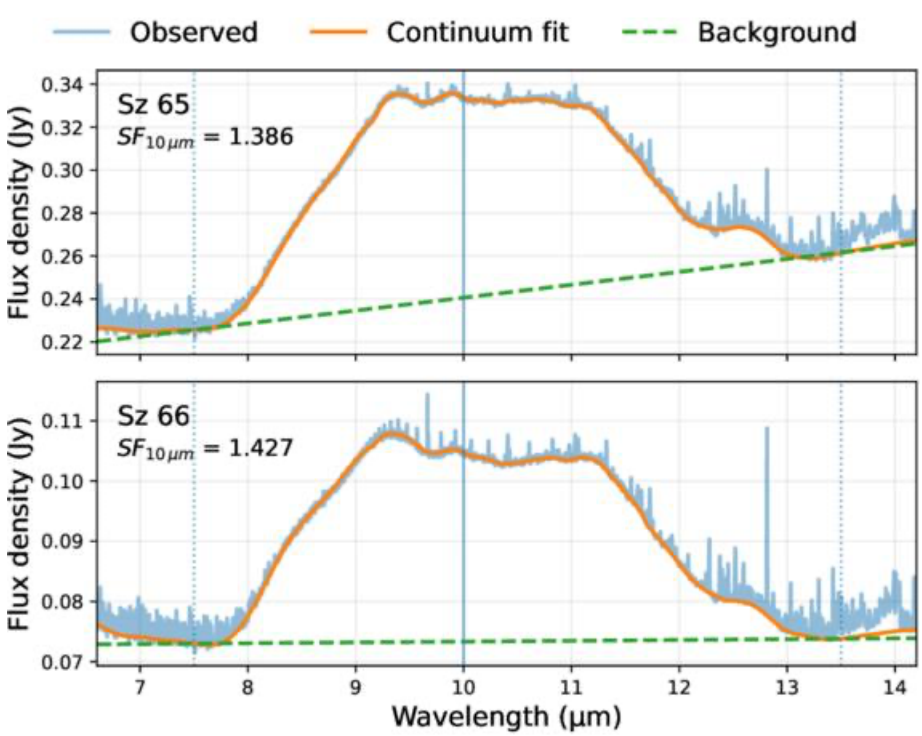

Figure 1: *The 10 µm silicate feature of the primary Sz 65 (upper), and the secondary Sz 66 (lower). The green dashed line shows the interpolated background from 7.5 to 13.5 µm.*

Volatile-rich Evolution of Molten Super-Earth L 98-59 d

Harrison Nicholls, Tim Lichtenberg, Richard D. Chatterjee, Claire Marie Guimond, Emma Postolec, Raymond T. Pierrehumbert

Nature Astronomy, 10, 809-817 (2026)

Small, low-density exoplanets are sculpted by strong stellar irradiation, but their primordial compositions and subsequent evolution are still unknown. Two often-considered scenarios hold that they formed with rocky interiors and H_2–He atmospheres (‘gas dwarfs’) or alternatively with bulk compositions dominated by H_2O phases (‘water worlds’). Here we constrain the possible range of evolutionary histories linking the birth conditions of low-density super-Earth L 98-59 d to recent observations using a coupled atmosphere–interior evolutionary model. We find that the observations can be explained by in situ photochemical production of SO_2 in an H_2 background, indicative of a chemically reducing mantle and substantial (>1.8 mass%) early sulfur and hydrogen content, inconsistent with both the gas-dwarf and water-world scenarios. L 98-59 d’s interior comprises a permanent magma ocean, allowing long-term retention of volatiles within its mantle over billions of years, consistent with California-Kepler Survey trends. Our analysis reveals an evolutionary pathway in which planets host volatile-rich atmospheres sustained by long-term magma-ocean degassing, shaped by secular cooling, atmospheric erosion and photochemistry. Internal and environmental processes contribute to the observed diversity of super-Earth and sub-Neptune exoplanets.

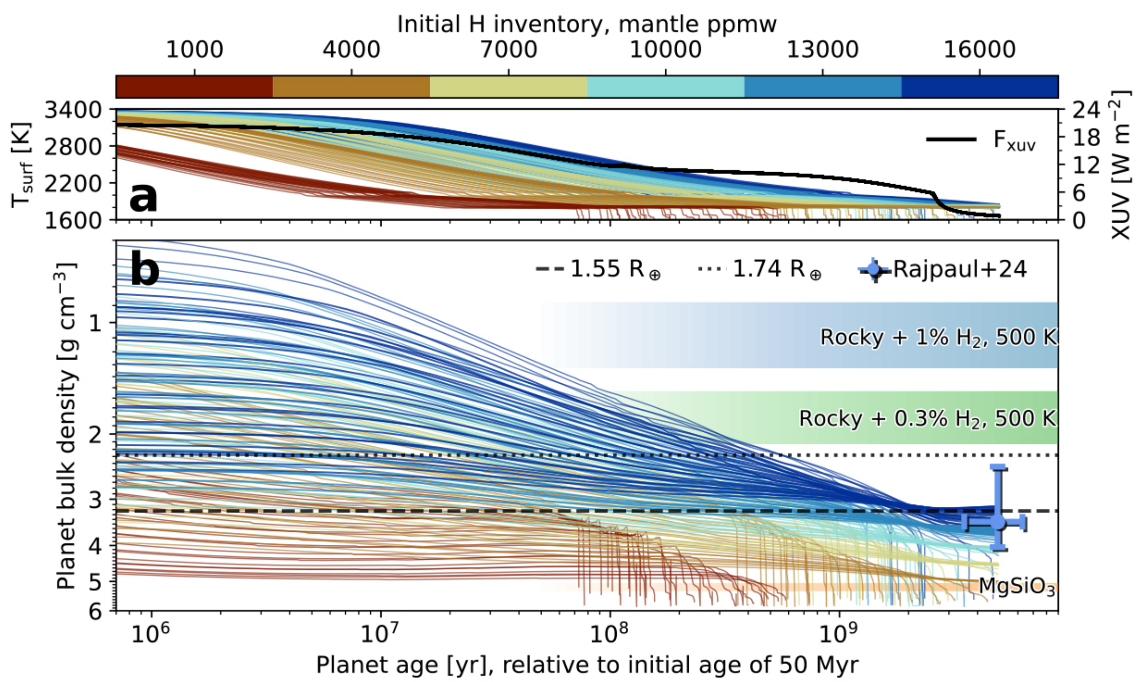

***Figure 1**: **a**, Initial hydrogen inventory (mantle ppmw) of each bulk-density evolution track is shown by the line colour. Blue/green shaded regions are reference densities for a planet of this mass[5]. Black dashed/dotted lines demarcate edges of the radius valley (at this planet mass) for low-mass stars. The region ±1σ compatible with the estimated bulk density of this planet is indicated by the blue error bar[15,24]. **b**, Evolution of surface temperature (coloured) and stellar XUV energy flux (black). For visual clarity, this figure only shows cases with S/H = 8.*

Hidden Gems in TESS: SHERLOCK Finds Two New Rocky Planets Around Nearby M Dwarfs

M. Timmermans, M. Dévora-Pajares, F. J. Pozuelos, K. Barkaoui , B. Rojas-Ayala, J. M. Almenara, S. B. Howell, A. H. M. J. Triaud , M. Gillon, M. G. Scott, Y. T. Davis, B. V. Rackham, A. J. Burgasser, X. Bonfils, K. A. Collins, B.-O. Demory, G. Dransfield, E. Ducrot, A. Fukui, M. Ghachoui, Y. Gómez Maqueo Chew, E. Jehin, N. Narita, P. P. Pedersen, R. P. Schwarz, G. Srdoc, S. Yalçınkaya, Z. Way

Monthly Notices of the Royal Astronomical Society, Volume 549, Issue 1, June 2026, stag710

The Hidden Gems project searches the TESS data for additional planets transiting low-mass stars in confirmed systems. Our goal is to identify planet candidates that are below the detection threshold set by the SPOC and QLP pipelines using sherlock, a specialized pipeline for robust detection and vetting of transit signals in TESS data. We present the discovery of two inner rocky planets in the TOI-237 and TOI-4336 A systems, validated with ground-based photometry from the TRAPPIST, SPECULOOS, ExTrA, and LCO facilities. TOI-237 c has a radius of 1.21 ± 0.04 $R_\oplus$, orbits its mid-M host star every 1.74 d, and is close to a 3:1 mean-motion resonance with TOI-237 b. TOI-4336 A c has a radius of 1.17 ± 0.06 $R_\oplus$, and orbits with a period of 7.58 d an M3.5 host star which is part of a hierarchical triple system. We performed model comparison to search for non-zero eccentricities and found that the circular transit models are statistically favoured. Dynamical simulations show that both systems are in stable configurations, and the transit timing variations expected for the TOI-237 system are of the order of seconds. TOI-237 c and TOI-4336 A c join the high-interest population of warm likely super-Earths below the so-called radius valley. In particular, TOI-237 c is a good candidate for phase curve observations with JWST/MIRI thanks to the small radius of the host star and its short period.

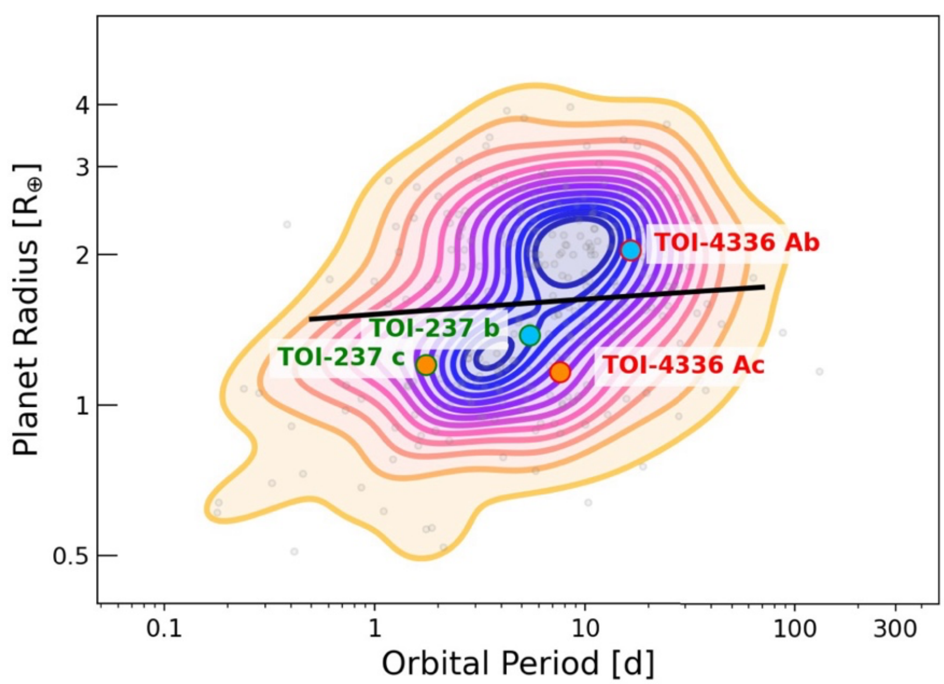

Figure 7: *Planet radius versus orbital period for transiting planets with radii $R_p < 4R_\oplus$ orbiting low-mass stars with T_{eff} < 4000K. Contours are kernel density estimates which highlight the density of these points. The radius valley is apparent from the bimodal distribution of the data. We illustrate its position with solid black lines, which are taken from R. Cloutier & K. Menou (2020). The planets of the TOI-237 system are labelled in green, the ones of the TOI-4336A system in red, with planets b marked as blue points and, planets c marked as orange points.*

Evidence for Systematically Larger Dust Grains in Upper Scorpius Relative to Taurus Disks

Yao Liu, Ilaria Pascucci, Fei Gao, Chengyan Xie, Feng Long, John Carpenter, Klaus M. Pontoppidan, Andrea Banzatti, Richard Booth, Steve Ertel, Min Fang, Uma Gorti, Tamara Molyarova

The Astrophysical Journal, Volume 1004, Number 2

Infrared spectroscopy provides a powerful diagnostic for probing the mineralogical properties of dust grains in the terrestrial planet–forming regions of protoplanetary disks. The Upper Scorpius association offers an excellent laboratory for studying disk evolution because it represents an evolved stage (5−10 Myr) compared with younger star-forming regions such as the Taurus molecular cloud (1−3 Myr). In this work, we present mid-infrared spectra of 11 disks in Upper Scorpius that were obtained with the Mid-Infrared Instrument aboard the James Webb Space Telescope. We derive emission feature indices for crystalline olivine and pyroxene centered at ~9.2 and ~11.1μm, as well as perform spectral decomposition to quantify dust crystallinity and characteristic grain size. These results are compared with those measured from Spitzer/IRS spectra of 31 disks in Taurus with similar stellar types. We find no significant difference in dust crystallinity between the two groups, suggesting that crystallization is largely established at early stages of disk evolution. Our analysis indicates that the average grain size in Upper Scorpius disks is systematically larger than that in Taurus disks, aligning with theories of dust evolution. We also observe a trend of increasing grain size towards later-type stars, as well as a correlation between crystallinity, grain size, and the flux ratio F_{24}/F_8, which serves as a measure of dust settling. These results suggest that dust processing proceeds in tandem with disk evolution.

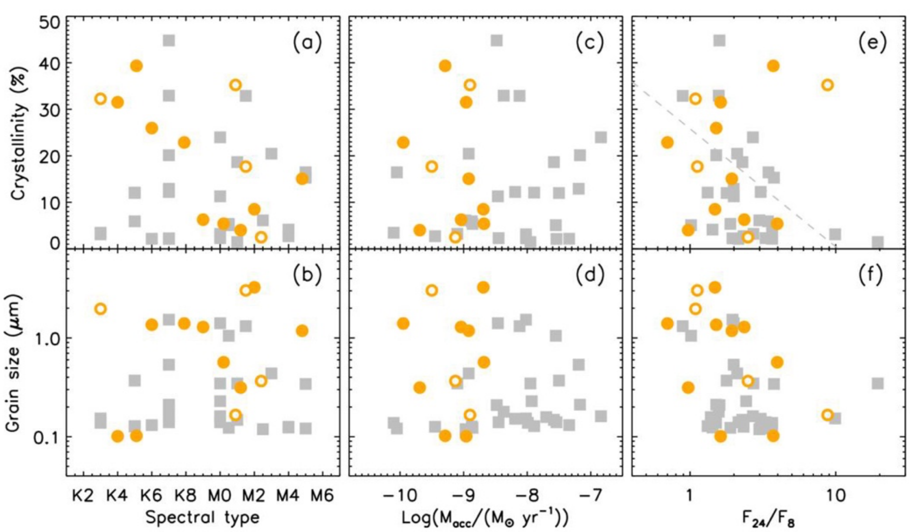

Figure 6*: Average sizes of amorphous grains (bottom panels) and crystallinity (upper panels) plotted versus the spectral type of the central stars (left column), accretion rate (middle column), and the flux ratio of* F_{24}/F_8 *as a measure of disk geometry (right column). As in Figure 3, gray squares represent Taurus disks, while orange dots and circles refer to USco disks around single stars and binaries, respectively. Table 2 summarizes the results of K-S tests that compare the distribution of crystallinity and grain size between the Taurus and USco sample. The Kendall's* τ *correlation coefficients and the corresponding* p-values *for each of the parameter pairs are provided in Table 3. The dashed line indicates a statistically significant trend (Kendall'ss* $P < 0.05$*).*

A Panchromatic JWST Spectrum of a Giant Starspot on the Fully Convective M Dwarf TOI-3884

C. A. Murray, L. Garcia, B. V. Rackham, Z. Berta-Thompson, A. D. Feinstein, S. J. Mercier, B. Charnay, L. Hebb, J. E. Libby-Roberts, Y. Rotman, A. Stephens, M. Timmermans, L. Welbanks, K. Barkaoui, Caleb I. Cañas, M. Delamer, E. Ducrot, S. Kanodia, S. Mahadevan, J. P. Ninan, and J. de Wit

The Astronomical Journal Letters, Volume 1003, Number 2

TOI-3884 b is a rare super-Neptune transiting a fully convective M dwarf that hosts a persistent giant polar spot. Because the planet occults this active region during every transit, the system offers a unique laboratory to directly probe the stellar surface and spot properties. We present seven James Webb Space Telescope (JWST) transits of TOI-3884 b observed with NIRISS and NIRSpec (spanning 0.6–5.3 μm. While all visits show a recurring spot-crossing signature, each transit exhibits a distinct spot-crossing morphology, enabling us to infer a stellar rotation period of P = 11.102 ± 0.003 days and tightly constrain the pole-on stellar orientation ($i_\star$ = 139:2 ± 0:3, $\lambda_\star$ = 31:1 ± 0:4, $\Psi_\star$ = 56:4 ± 0:3) and spot properties ($R_{\rm spot}$ = 0.576 $^{+0.006}_{-0.005}$ ⋆, $R_\star$, $\varphi_{\rm spot}$ = −84:69 ± 0:12). We leverage this orbital configuration to measure the first empirical panchromatic spectrum of an M dwarf starspot with JWST, establishing a direct observational benchmark for stellar atmosphere models in the fully convective regime. Comparison with 1D NewEra and SPHINX atmosphere models indicates that the spot is 183 ± 1 K cooler than the photosphere, consistent with previous ground-based measurements and expectations for mid M dwarf spot contrasts. While the models reproduce the observed contrasts at wavelengths longer than 1μm, they significantly underpredict the contrasts at shorter wavelengths. These results demonstrate that M dwarf stellar atmosphere models may not fully capture the wavelength dependence of stellar contamination in transmission spectra and highlight the importance of empirical spot spectra for robust interpretation of planetary atmospheres, particularly in the optical.

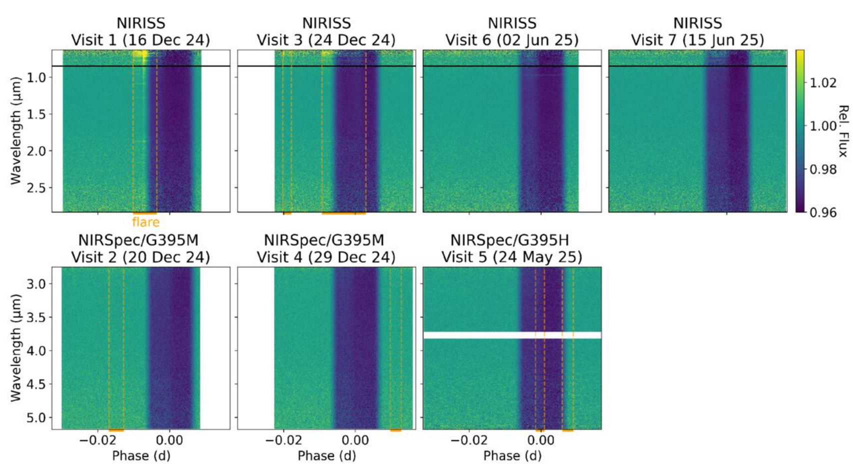

Figure 1: Spectroscopic time series of the transit light curves of TOI-3884 b for all seven JWST visits, reduced with ExoTEDRF (Section 2.2). NIRISS/SOSS observations are presented in the top row, and NIRSpec/BOTS in the bottom. Each panel shows normalized flux as a function of orbital phase and wavelength, and the color scale is shared across all panels. In all visits, the planetary transit appears as a broad vertical band centered at phase zero, and the spot-crossing event is apparent in the first half of the transit. Several visits also exhibit continuum and line emission attributable to stellar flares. The horizontal black lines (0.85 μm) on the top panels indicate approximately where NIRISS orders 1 and 2 overlap (0.85–1.10 μm). The white horizontal bar in Visit 5 indicates the gap between the NRS1 and NRS2 detectors for the G395H mode (3.72–3.82 μm); in the G395M mode, only NRS1 is illuminated. The timings of identified flares are marked in orange on the x-axes.

From Young to Older Disks: JWST/MIRI Evidence for Fading Molecular Emission and Hints for Elevated C/O in Upper Scorpius

Chengyan Xie, Ilaria Pascucci, Feng Long, Uma Gorti, Andrea Banzatti, Richard Booth, Klaus Pontoppidan, Tamara Molyarova, John Carpenter, Min Fang, Yao Liu, Eshan Raul, Ke Zhang, Steve Ertel, Jordan Stone, Aaron Empey, Carlo F. Manara, Paola Pinilla, Colette Salyk, Benoit Tabone, Miguel Vioque, Lucas Cieza, Giovanni Rosotti, James Miley, Geoffrey A. Blake, Abygail Waggoner

Astro-ph.EP: arXiv:2606.27477

We present JWST/MIRI spectroscopy of 14 disks in the older (~5-10 Myr) Upper Scorpius (USco) association and use slab of gas in local thermal equilibrium to infer basic gas properties. We find that half of these disks are molecular rich, with detections of H_2O, CO_2, HCN, C_2H_2, and H_2, while the other half are molecular poor, showing no molecular emission other than H_2. We further combine this sample with 10 other USco disks from the AGE-PRO program and compare the combined older sample to young (~1-3 Myr) JDISCS Cycle~1 systems, which are analyzed in a similar manner. We find that USco disks have lower detection rates of major molecular species but a significantly higher detection rate of rarer C-bearing molecules such as C4H2. At a given accretion luminosity, molecular line luminosities are systematically lower in USco than in young disks, and the scaling relations with accretion luminosity differ between the two populations. Moreover, we find that about half of the older disks, preferentially the millimeter faint, and likely more compact disks, have observable mass ratios of C- to O-bearing molecules that are higher than the maximum values in the young sample. These results point to reduced inner-disk molecular gas masses, cooler emitting layers, and higher inner gas C/O ratios in older disks, the latter being consistent with pebble drift. Taken together, our findings provide evidence for chemical evolution of inner disk gas from young to older systems, with important implications for the accretion of primordial planetary atmospheres.

***Figure 11**: Upper panel: Comparison of average spectra from the young JDISCS C1 sample, very low mass star (VLMS, M∗ < 0.2M⊙, representative of C/O ratio > 1) disks (Grant et al. 2025), and the mm-bright (MR1–MR3) and mm-faint (MR5–MR7) disks in the U2970 sample which has the same spectral type as JDISCS C1. The mm-bright USco average spectrum closely resembles the average JDISCS C1 spectrum.*

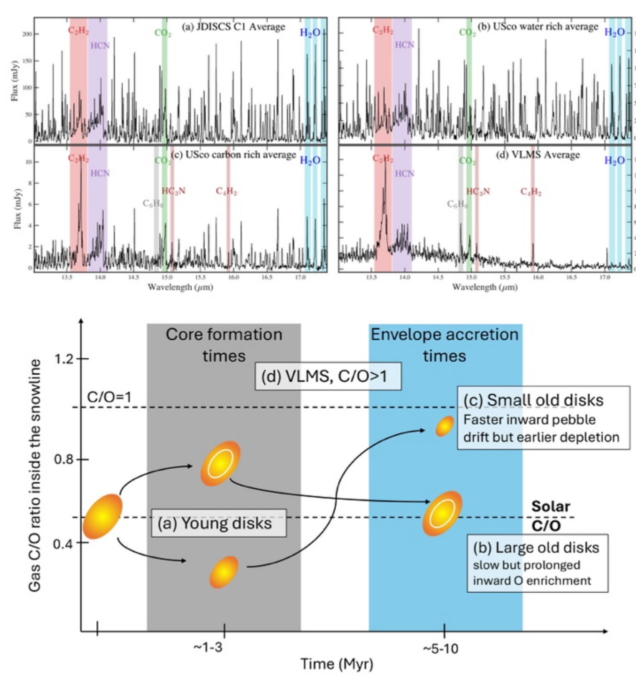

In contrast, the mm-faint average USco spectrum shows less water and stronger emission from C-bearing molecules but not at the level of the VLMS average spectrum. This suggests an elevated C/O ratio relative to the water-rich disks, but still below 1.

Lower panel: Sketch of the proposed scenario for explaining the behavior, with (a) to (d) corresponding to the four subplots in the upper panel.

Probabilistic Spectral Reconstruction of Trans-Neptunian Objects from Sparse Photometry: A Framework for Taxonomy, Survey Optimization, and Outlier Detection

Hsing Wen Lin (林省文), Larissa Markwardt, Kevin J. Napier, Fred C. Adams, Renu Malhotra, David W. Gerdes

The Astronomical Journal, Volume 171, Number 6

Near-infrared (near-IR) spectroscopy provides critical constraints on the surface composition of trans-Neptunian objects (TNOs), but spectroscopic observations remain limited compared to broadband photometry. We develop a probabilistic latent-space framework to quantify how much spectral information is retained in sparse photometric measurements. Using a principal component representation trained on a sample of near-IR spectra, we model the spectral manifold of TNOs and perform Bayesian inference in this reduced space to reconstruct full spectra from photometry while propagating measurement uncertainties. Leave-one-out cross-validation demonstrates that the dominant modes of spectral variability are low dimensional: approximately four to five principal components capture the structure relevant for taxonomic classification, while 8–10 components improve spectral reconstruction fidelity and uncertainty calibration. For most objects, the reconstructed spectra achieve empirical credible interval coverage of ~95% across the wavelength. These results suggest that the diversity of near-IR spectral shapes in the current sample is governed by structured, correlated surface processes rather than stochastic variation. Practically, we apply this framework to survey optimization, quantifying the information content of JWST/NIRCam filters to identify optimally informative configurations (e.g., F090W, F115W, F410M, F460M) for future observations for TNO taxonomy. Additionally, we demonstrate the pipeline's capability to detect and reconstruct rare spectral types, such as the peculiar Neptune Trojans 2006 RJ_{103} and 2011 SO_{277}, by allowing constraining photometry to select low-probability intermediate models from the continuous topological manifold. Ultimately, this framework bridges the gap between sparse photometry and spectroscopy, providing a statistically rigorous tool to map the compositional structure of minor planets in upcoming large-scale surveys.

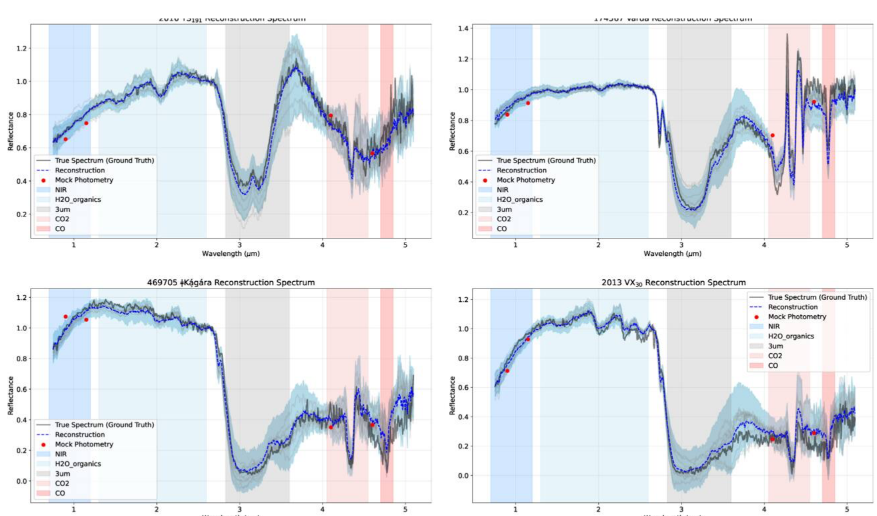

***Figure 6**: Reconstructed spectra for four distinct TNO spectral types. The spectra of the two Neptune Trojans, 2010 TS_{191} and 2013 VX_{30}, were withheld from the traiing seeds to test generalization. The two TNOs 174567 Varda and 469705 =| Kagara were reconstructed using an LOOCV framework. The shaded regions indicate the 95% posterior credible intervals, while the gray lines represent 10 alternative realizations randomly sampled from the posterior. Major absorption features (3 μm , H_2O, CO_2, CO) are highlighted.*

Coupled atmospHere Interior modeL Intercomparison (CHILI)–Protocol Version 1.0: A CUISINES Intercomparison Project of Magma Ocean Models

Tim Lichtenberg, Laura Schaefer, Joshua Krissansen-Totton, Yamila Miguel, Denis E. Sergeev, Philipp Baumeister, Jessica Cmiel, Leoni J. Janssen, T. Giang Nguyen, Yoshinori Miyazaki, Harrison Nicholls, Alexandra Papesh, Hugo Pelissard, Bo Peng, Junellie Perez, Emma Postolec, Mariana Sastre, Arnaud Salvador, Hanno Spreeuw, Andrea Zorzi, Thomas J. Fauchez, Keiko Hamano, Jérémy Leconte, Maxime Maurice, Lena Noack and Laurent Soucasse

The Planetary Science Journal, Volume 7, Number 5

Spectroscopic characterization of rocky exoplanets with the James Webb Space Telescope has brought the origin and evolution of their atmospheres into the focus of exoplanet science. Time-evolved models of the feedback between interior and atmosphere are critical to predict and interpret these observations and link them to the solar system terrestrial planets. However, models differ in methodologies and input data, which can lead to significant differences in interpretation. In this paper, we present the experimental protocol of the Coupled atmospHere Interior modeL Intercomparison (CHILI) project. CHILI is an (exo)planet model intercomparison project within the Climates Using Interactive Suites of Intercomparisons Nested for Exoplanet Studies (CUISINES) framework, which aims to support a diverse set of multimodel intercomparison projects in the exoplanet community. The present protocol includes the initial set of participating magma ocean models, divided into evolutionary and static models, and two types of test categories, one focused on solar system planets (Earth and Venus) and the other on exoplanets orbiting low-mass M dwarfs. Both test categories aim to quantify the evolution of key markers of the links between planetary atmospheres and interiors over geological timescales. The proposed tests would allow us to quantify and compare the differences between coupled atmosphere–interior models used by the exoplanet and planetary science communities. Results from the proposed tests will be published in dedicated follow-up papers. To encourage the community to join this comparison effort, and as an example, we present initial test results for the early Earth and TRAPPIST-1 b, conducted with models differing in the treatment of energy transport in the planetary interior and atmosphere, surface boundary layer, geochemistry, and in- and outgassing of volatile compounds.

__Figure 1__: Illustration describing the processes treated by several models participating in CHILI. The leftmost six models are evolutionary, where dynamics and composition change with time. The rightmost four models are static, where the planets are implicitly assumed to be at steady state. MORE is shown between evolutionary and static models, as it is not fully time dependent (see main text). The six radial domains of the models include the core, solid mantle, liquid mantle, surface boundary layer, atmosphere, and exosphere or outer space. Interactions coupling these layers are denoted by arrows.

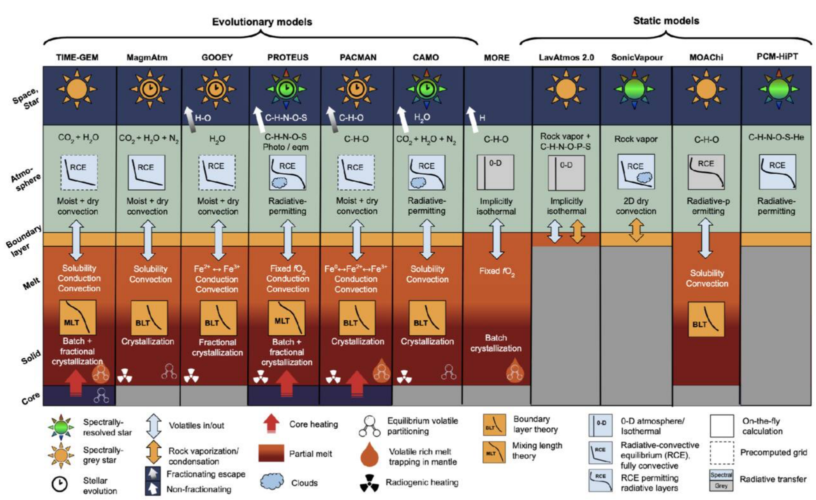

A Gem System with a Lava World and a Habitable Zone Sub-Neptune Orbiting TOI–1752

A Peláez-Torres, F J Pozuelos, G Morello, M Dévora-Pajares, K Barkaoui, L Gkouvelis, E Pallé, K A Collins, B V Rackham, S Geraldía-González, M Centenera-Merino, R Varas, E Esparza-Borges, Z Parlapani, J Flores, J Aceituno, P J Amado, A Burdanov, Y Calatayud-Borras, D R Ciardi, B O Demory, T Gan, S Giacalone, M Gillon, Y Gómez Maqueo Chew, K Kawauchi, A Khandelwal, J Korth, M Lendl, J P de Leon, J Livingston, N Morales, F Murgas, N Narita, J L Ortiz, H Parviainen, M Pichardo Marcano, I Plauchu-Frayn, D Queloz, D Rapetti, J Saito, A Sánchez-López, A B Savel, R P Schwarz, U Schroenegger, M Serra-Ricart, C Stockdale, A H M J Triaud, J de Wit, F Zong Lang

Monthly Notices of the Royal Astronomical Society, Volume 548, Issue 3, May 2026, Stag713

The Transiting Exoplanet Survey Satellite (TESS) has delivered a large number of transiting planet candidates around nearby stars by identifying periodic decreases in stellar brightness. Establishing the planetary nature of these signals and determining their fundamental properties is a necessary step towards detailed studies of their internal structure, atmospheres, and formation pathways. In this work, we investigate the planetary nature of the TOI-1752 system (M1 V, 103.02 ± 0.34 pc), which hosts two TESS candidates: TOI–1752 b, a short-period object consistent with a lava-world scenario, and TOI–1752 c, a sub-Neptune-size planet candidate located in the optimistic habitable zone. We obtained ground-based multicolour photometric follow-up observations of TOI–1752, which we combined with TESS photometry to assess the nature of both signals. We performed a formal statistical validation using the TRICERATOPS framework, while independently vetting the candidates with the neural-network-based classifier WATSON-Net, which provides a machine-learning assessment of their planetary likelihood based on light-curve morphology, centroid diagnostics, and auxiliary vetting features. We validate TOI–1752 b as a bona fide planet with a radius of 1.69 ± 0.07 $R_\oplus$ and an orbital period of $0.935186^{+0.000001}_{-0.000002}$ d, and TOI–1752 c with a radius of $2.29^{+0.13}_{-0.14}$ $R_\oplus$ and an orbital period of 32.7144 ± 0.0004 d. The combined analysis confirms TOI–1752 as a new planetary system, places TOI–1752 c within the optimistic habitable zone of its host star, and identifies TOI–1752 b as a promising target for atmospheric characterization, with an estimated emission spectroscopy metric of up to ~ 8.

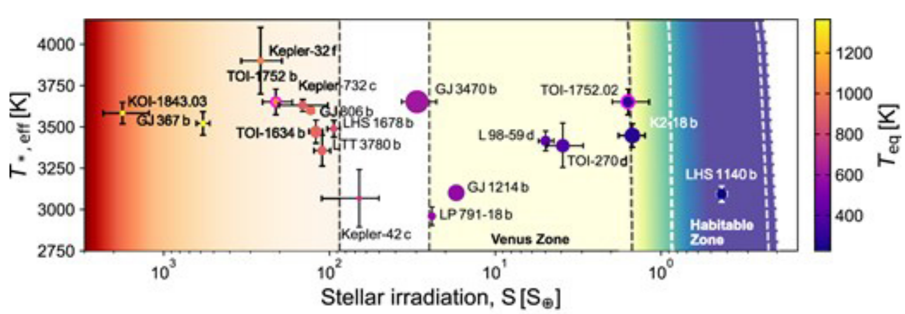

Figure 10: Stellar irradiation comparison between TOI–1752 planetary system (circled in pink), the sub-Neptune sample defined by N. Madhusudhan et al. (2025), and the sample of USP planets orbiting M dwarfs that are hosted within a multiplanet system, with scaled planetary radii. Planets are coloured as a function of the T_{eq}. The Venus Zone (VZ) (yellow shade; S. R. Kane, R. K. Kopparapu & S. D. Domagal-Goldman 2014) and HZ (blue shade) transition gradually, influenced by complex climate feedback mechanisms that can drive planets toward either Earth-like or Venus-like states within this orbital range (D. Quirino et al. 2023). The HZ greenhouse variation is represented by the recent Venus, runaway greenhouse, moist greenhouse, maximum greenhouse, and early Mars layers (white dashed lines; R. K. Kopparapu et al. 2013). We also indicate the insolation threshold beyond which the surfaces of planets are expected to melt (the black dashed line on the left; M. Zilinskas et al. 2022).

The Goldilocks Problem for Detecting Water in Terrestrial Planets: Constraining Water Abundances in the Mid-infrared with LIFE

S. Rugheimer, E. Alei, B.S. Konrad, B. Taysum, J. L. Grenfell, T. Lichtenberg, D. Kitzmann, F. van der Tak, S.P. Quanz, and LIFE collaboration

The Astrophysical Journal, Volume 1003, Number 1

We investigate how well the Large Interferometer for Exoplanets (LIFE) mission concept can detect habitable conditions on exoplanets through the presence of atmospheric water vapor as a proxy for surface oceans. We model the atmosphere of a prebiotic Earth-like planet across a range of water concentrations, from water-poor to water-rich, with surface partial pressures from 10^{-7} to 1 bar of H_2O. We simulate LIFE-like noise at spectral resolutions *R* = 50 and 100 using LIFEsim and perform Bayesian atmospheric retrievals to determine the technical requirements for LIFE to confirm habitability. We model three vertical water distributions—a vertically constant profile, a Manabe–Wetherald-based Earth-like profile, and a diffusion and photochemistry profile—to test how the assumed vertical structure influences the retrieved abundances. Clouds are not modeled. We find the ability for LIFE to detect water strongly depends on the vertical profile assumed. LIFE is unable to constrain the highest-water cases and provides upper limits on low-water planets. For the highest-water abundances, absorption features saturate and reduce the sensitivity for characterizing precise H_2O levels. Water vapor is not detectable in any profile modeled for $\leq 10^{-6}$ bar in surface water, comparable to Mars. For an Earth-like profile, LIFE could constrain H_2O concentrations from $\sim 10^{-3}$ to 1 bar, spanning below and above present-day Earth concentrations of 10^{-2} bar. Detectable atmospheric water may imply surface oceans, as water is highly reactive and rapidly removed by surface mineral reactions. Thus, LIFE can characterize water abundances indicative of habitable surface conditions.

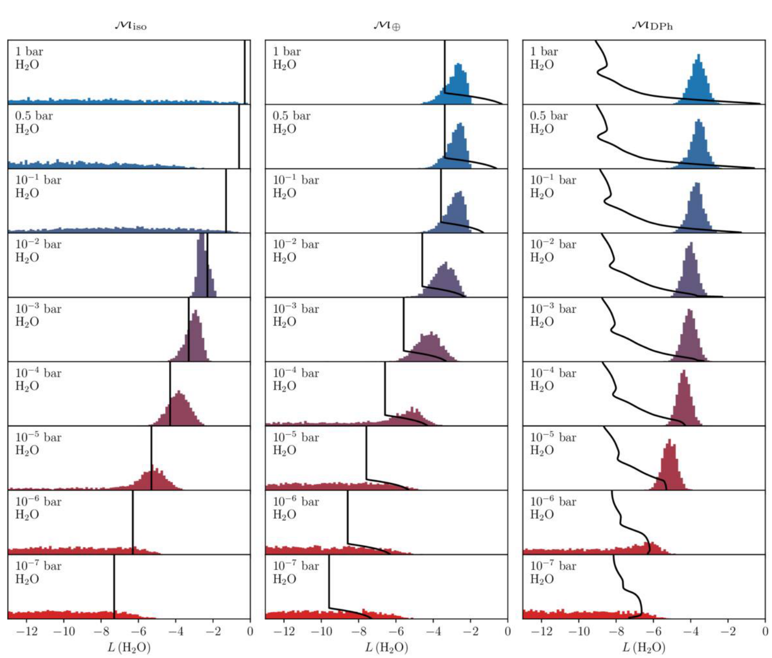

***Figure 4**: Water posteriors for simulations for a range of surface H_20 abundances from 1 bar to 10^{-7} bar at a resolution and S/N of R = 100 and S/N = 10, respectively. The black lines are the H_20 profiles in volume mixing ratios in log10 (L) overlaying the H_20 posteriors. The left panel assumes an altitude-invariant profile of water, commonly used in retrievals. The center panel fixes the surface abundance and then assumes a scaled Earth-like profile. The right panel fixes the surface H2O abundance and has diffusion and photochemical production at all other altitudes.*

NSF-DOE Vera C. Rubin Observatory Observations of Interstellar Comet 3I/ATLAS (C/2025 N1)

Colin Orion Chandler, Pedro H. Bernardinelli, Mario Jurić, Devanshi Singh, Henry H. Hsieh, Ian Sullivan, R. Lynne Jones, Jacob A. Kurlander, Dmitrii Vavilov, Siegfried Eggl, (See article for full author list)

The Astrophysical Journal Letters, Volume 1001, Number 2

We report on the observation and measurement of astrometry, photometry, morphology, and activity of the interstellar object 3I/ATLAS, also designated C/2025 N1 (ATLAS) with the NSF-DOE Vera C. Rubin Observatory. Comet 3I/ATLAS, the third known interstellar object, was discovered on UT 2025 July 1. Rubin Observatory had coincidentally collected images of the object's region of the sky during routine commissioning. Facilitated by Rubin's high resolution and large aperture, we successfully recovered object detections from Rubin observations spanning UT 2025 June 21 (10 days before discovery, when 3I/ATLAS was 4.5 au from the Sun) through the date of discovery, and we acquired additional images through UT 2025 July 20 as part of commissioning. We measure on-sky locations of 3I/ATLAS in Rubin *ugrizy* bands, with a typical precision of ~70 mas, and briefly describe the reason this is coarser than our measured static source astrometric precision of ~3 mas in Rubin images. We measure *grizy* magnitudes of 3I/ATLAS photometry at ~0.01 mag precision, detecting no short-term photometric variability above 0.01 mag. We derive an estimated near-nucleus dust-to-nucleus scattering cross-sectional ratio of $\eta \gtrsim 13$ on UT 2025 July 2 based on Rubin photometry and an upper limit nucleus size computed from Hubble Space Telescope observations. We find Rubin colors of $g - r =$ (0.657 ± 0.013) mag, $r - i =$ (0.235 ± 0.018) mag, $i - z =$ (0.147 ± 0.042) mag, and $z - y =$ (0.047 ± 0.052) mag. These data represent the earliest observations of this object by a large (≳8 m class) telescope and illustrate the type of measurements (and discoveries) Rubin's Legacy Survey of Space and Time will provide after it begins in early 2026.

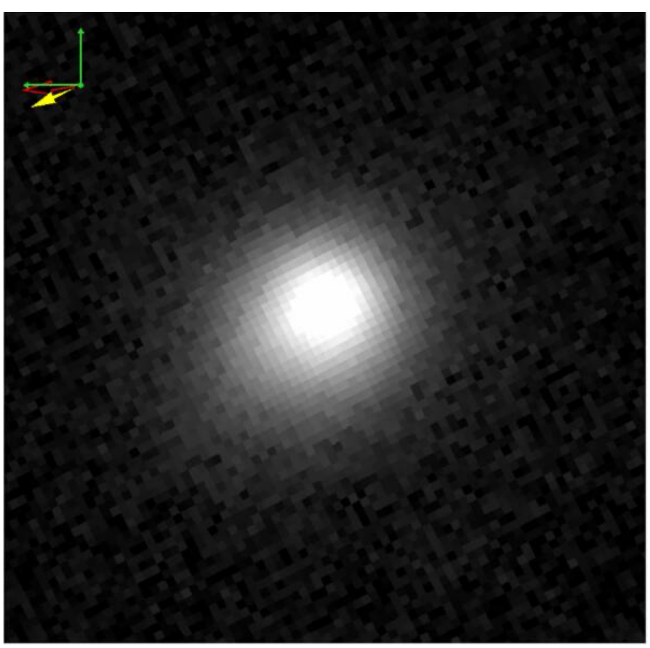

Figure 1: *3I/ATLAS minimum coaddition from UT 2025 July 3, 21 × 30 s r-band images acquired by NSF-DOE Vera C. Rubin Observatory. The field of view (FOV) is ~15" × 15", with north up and east left. The antisolar (yellow arrow) and antimotion (red-outlined black arrow) directions are shown.*